Preparing for Virtual Testing for Crashworthiness: Proposing a Method for Certifying ATD Models for Frontal Crash Assessments

Manuel Valdano, Martin Östling, Linda Eriksson, Francisco J. López-Valdés, Bengt Pipkorn

Abstract In the Euro NCAP 2030 roadmap, Virtual Testing using the H3 adult ATD FE-models is planned to be implemented in the next phase. Certification of ATD models ensures that the virtual models can predict the response of the mechanical counterpart at an acceptable level of accuracy. The aim of this study was to develop an open-source generic frontal impact sled FE-model and method that can be used to certify H3 adult ATD models for Virtual Testing. The method included two crash pulses corresponding to 40 and 56 km/h full-frontal rigid barrier crashes. An objective rating metric based on the ISO/TS-18571 was used to determine model correlation. Six simulations were conducted, and the predictions were compared to the results from 18 physical tests. A fair-to-good correlation (0.757-0.810) was observed for all simulations, with a similar correlation at both crash pulses for each ATD model. Although the H35F and H350M models had the best correlation, the H395M model had a fair rating. A good correlation (0.832-0.856) was observed for the sled measurements, with no significant differences between ATDs and crash pulses. This model and method could be a part of the H3 adult ATD model certification to be used for Virtual Testing.

Keywords Certification, frontal crashes, Euro NCAP, Hybrid III, Virtual Testing.

I. INTRODUCTION

The automotive industry has used numerical simulations for decades to complement crash testing for product development, minimising the number of crash tests necessary to study and optimise new products. The European New Car Assessment Programme (Euro NCAP) started the integration of Virtual Testing Crashworthiness (VTC) into vehicle ratings in 2009 for pedestrian protection. In 2023, Euro NCAP announced the implementation of Virtual Testing in their assessment protocols, with the far-side occupant assessment aimed at enhancing assessment robustness through the use of WorldSID models. This development, set to be implemented from 2024 onwards in a monitoring stage and fully enforced by 2026, underscores a paradigm shift towards leveraging computational models to complement physical testing. Euro NCAP's initiative not only signifies a broader scope for assessments but also addresses limitations in physical test scenarios, ensuring a more comprehensive and real-world-like evaluation approach.

Euro NCAP has proposed a new frontal impact VTC in their roadmap for 2030. This aims to enhance the evaluation of frontal protection by deploying additional virtual simulations. These simulations will be based on variations of load cases from the Euro NCAP frontal sled procedure as defined in the Euro NCAP Frontal Occupant Test & Assessment protocol [1]. The simulations will also include a family of Hybrid III (H3) finite element (FE) anthropometric test device models to account for occupant variability in occupant protection.

To ensure reliable and robust virtual testing according to the industry standard, the models used in VTC, i.e., human body models (HBMs) and ATDs, must be assessed for their validity and capabilities, and the quality of the model predictions have to be certified. This assessment is conducted in three stages [2]. Firstly, the general model properties are checked by comparing the mass and dimensions of the components and the entire ATD with their physical counterparts. Secondly, the fundamental dynamic behaviour of the model is verified by carrying out validation test procedures similar to those done on the physical ATD. Lastly, an application-specific assessment is performed by comparing the components and the entire ATD with the predictions of their physical counterparts

M. Valdano (e-mail: mvaldano@comillasedu; tel: +34 644 64 05 53) is a PhD. student and F. J. López-Valdés is Associate Professor and Researcher at MOBIOS Lab, IIT, Universidad Pontificia Comillas, Madrid, Spain. B. Pipkorn is Adjunct Professor at Chalmers University and Director of Simulation and Active Structures at Autoliv Research, Vårgårda, Sweden. Martin Östling is a Senior Research Specialist and Linda Eriksson is a Senior CAE specialist at Autoliv Sweden, Vårgårda, Sweden.

for simplified loading conditions. These conditions use load levels and patterns similar to those observed in the final conditions where the ATD model will be used for Virtual assessment. Since the introduction of VTC for pedestrian protection, certification procedures for pedestrian models have been introduced [3]. Furthermore, a certification procedure was also developed for far-side impact VTC and WorldSID ATD [4,5].

Following the Euro NCAP 2030 roadmap, the H3 models must be validated at component, sub-assembly and full-body levels to be used in the frontal impact VTC. Validation setups for thorax and neck validation were presented by [6]. Using the setups, the validation of the 50th percentile male H3 and 50th percentile male THOR ATD models were assessed. For full body validation, boundary conditions (restraint system) similar to the boundary conditions the model will experience in product development or consumer information programmes, are necessary. The boundary conditions in a sled setup are a seat, seat belt system and airbag. Sled tests were carried out to validate the 5th percentile female and 50th percentile male H3 ATD by the Automotive Occupant Restraints Council (AROC) [7]. However, boundary conditions used in the test setup were not clear and limited results from the tests were published. Therefore, there is a need for sled test data in a simple generic environment with clear boundary conditions that can be used to validate the family of adult H3 ATD models.

The aim of the study was to develop an open-source generic frontal impact sled FE-model and a method that can be used in full-body certification of the family of adult Hybrid III ATD models to be used for Virtual Testing in frontal crashes.

II. METHODS

The development of the open-source generic frontal impact sled FE-model used to certify the family of adult Hybrid III ATD models was based on the experimental results obtained in a series of 18 physical tests [8]. These tests were conducted utilising the Hybrid III 5th percentile female (H35F), 50th percentile male (H350M), and 95th percentile male (H395M) ATDs. The tests were performed using generic crash pulses developed to represent 40 km/h and 56 km/h full-frontal rigid barrier crashes [9]. Each configuration was repeated three times to enable evaluation of the repeatability of the test setup. Three ATD FE models were positioned mimicking the position of the physical counterparts, and a 3-point belt system was used with a double pretensioner (retractor and lap belt anchor), load limiter, and crash-locking tongue. An objective rating metric based on the ISO/TS 18571 [10] was utilised to evaluate the correlation between the test results and the FE model predictions.

Test Setup for Physical Tests

A generic frontal system sled was used to perform 18 tests [8]. The seat used in the sled setup was a semi-rigid seat developed by [11]. A rigid seatback with an 18° orientation to the vertical was used, and a 45°-foot support was employed as well. The restraint system used in the generic frontal system was a B-pillar installed 3-point belt system, a driver airbag, and a generic knee bolster. Anchor points for the 3-point belt system were based on a mid-size European vehicle [12]. The belt system was comprised of a 2 kN double pretensioner in the retractor and lap belt anchor, a 4 kN load limiter in the retractor, and a crash-locking tongue. The seatbelt webbing had a constant width of 47 mm and a tension of 11.5 kN at 10% elongation. A driver airbag was mounted on a steering wheel with a collapsible column. The generic knee bolster had a foam thickness of 100 mm mounted to a rigid plate. Two generic crash pulses representing 40 km/h and 56 km/h full frontal crashes were used to impulse the generic frontal system. The time vs. sled acceleration of the two crash pulses can be observed in Fig. 1.

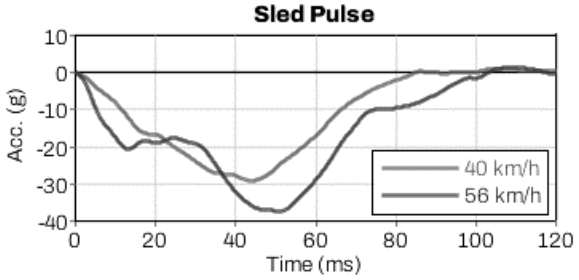

Fig. 1. Time vs sled acceleration of the crash pulses at 40 km/h and 56 km/h used to perform the tests with the generic frontal system.

The tests were conducted using three H3 ATDs manufactured by Humanetics Innovative Solutions, Inc., one per ATD size. The ATDs were seated in an upright posture with their hand on the steering wheel. The seat coordinate system origin was defined as shown in Fig. A1, which was used to measure the position of the ATD

and the environment.

The H350M and H395M were tested in the same setup, i.e., the seat, footrest, belt anchors and steering wheel were in the same position. The setup was changed for the H35F, where the seat and footrest were moved. The seat was moved 100 mm forward and 25 mm upwards relative to the position used with the H350M. This displacement included coordinate system origin. The foot support was moved 40 mm rearwards and 22 mm upwards.

The position and complete test set-up for the three ATDs were 3D scanned using a FARO arm device before conducting the test. These scans focused on the ATD, seatbelt, steering wheel, footrest, and seat. This was done to ensure precise positioning and accurate replication of the belt routing across the thorax and pelvis in the simulation model.

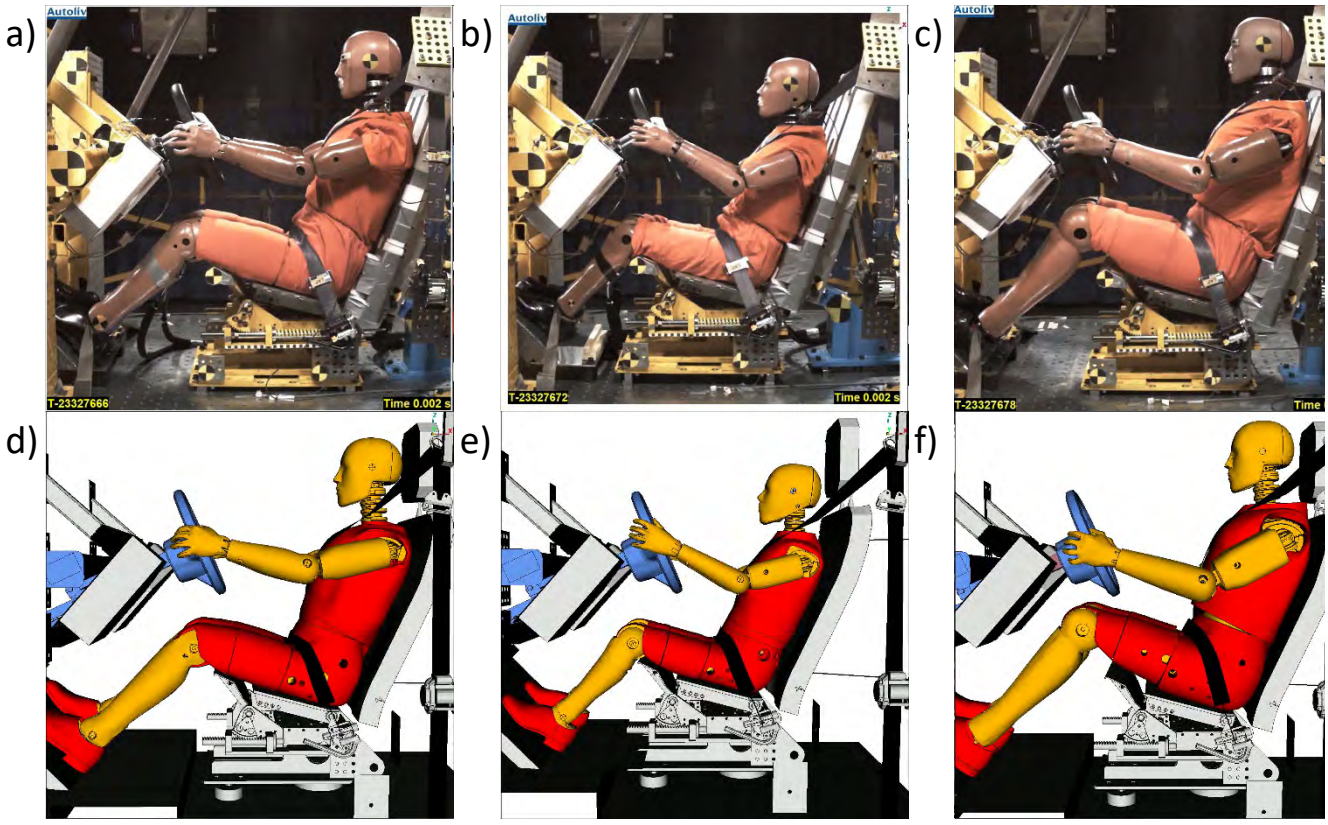

Fig. 2. Pictures of the ATD position for: a) H350M in the test, b) H35F in the test, c) H395M in the test, d) H350M in the simulation, e) H35F in the simulation, and f) H395M in the simulation.

Onboard high-speed cameras recorded the tests at a frequency of 1000 Hz. These cameras captured images of the left and right-side overview, a top and front view, and detailed views of the pelvis and its interaction with the seat, lap belt, lap belt pre-tensioner, buckle, and crash locking tongue. A frequency of 20 kHz was used to capture the ATD and sled measurements. A description of these signals and their filtering can be observed in Table AI and Table AII in the Appendix.

FE Model of Test Setup

A generic frontal impact sled model mimicking the physical was set up for this study based on the model from [12]. Activation times of the pre-tensioners and airbag matched those of the physical test. A generic retractor model was tuned to match webbing pay-in, pay-out and forces in the retractor and lap belt anchor, which are the points where a pretensioner and/or a load limiter were used. Bending beams [13] were used in the lap and shoulder belts to avoid excessive bending.

Three ATD FE models were used to carry out the simulations, each one corresponding to its physical counterpart. These ATDs were obtained from Humanetics Innovative Solutions, Inc. and were the Harmonized Hybrid III LS-DYNA Models. The versions of these ATDs were v1.5.1 for the 50%, v2.0.2 for the 5%, and v1.0.2 for the 95%. Fig. 2 shows the position of the three ATD sizes and their FE model counterpart.

The Oasys suite v19.1 and BETA CAE suite v23.1.0 were used as pre- and post-processors, respectively, for the simulations. All simulations were carried out using LS-Dyna MPP 971 single precision R9.3.1.140922 and 32 CPUs for all simulations. A time step of 0.7 µs was used with a simulation length of 140 ms. The ATD certification

protocol for far-side impacts [14] defines the minimum simulation time as the time of maximum head excursion in the y axis + 20%. Thus, the analysis and correlation time window used was 120 ms, which is the time of the maximum head excursion in the x-axis + 20%, based on the H395M criteria for the worst-case scenario.

Positioning and Seatbelt Fitting Procedure

The family of H3 ATDs was positioned using the marionette method by pulling different body parts of the ATD with springs until the surface of the ATD model was matching the surface of the 3D scanning. The final position of the ATDs was obtained following the next procedure. Initially, the H-point and pelvis angle were set to match the orientations reported from tests. Next, control surfaces obtained from 3D scanning were used to obtain the position of the model's legs, thorax, head, and upper arms. Then, a pre-simulation was used to reach the final position of the model in three stages. First, the legs, thorax, and head were pulled to their final positions within 75 milliseconds, ensuring the hands touched the steering wheel. Following this, the model's arms were positioned into their final posture over another 75 milliseconds. Lastly, the model was then allowed to stabilise over 50 milliseconds, employing a global damping factor of 0.1. A 150 ms simulation was run using the positioned ATD model to check that the position was stable. Reference foam was activated for the pelvis flesh, and vertical displacements of the pelvis were tracked. If any displacement exceeding 3 mm was observed, the positioning process was repeated to avoid such displacement.

The seatbelt was fitted using Oasys Primer. Points throughout the 3D scanned seatbelt were taken to fit the FE belt to ensure a close position match with the test data. Extra points were taken to match the position of the seatbelt load cells, including the orientation of the belt section around these points.

Known points and orientations of seatbelt sections from the lap belt were also used to fit this belt section. This avoided excessive bending around the leg-abdomen area using a fitting process without these constraints. Extra belt around the buckle and the lap belt anchor were included to match the belt pay-in when the pre-tensioners were fired.

A time-dependent friction coefficient calibrated from the experimental data was used between the seatbelt webbing and the D-ring. This was the result of observing the belt bunching around the D-ring in the physical tests. The time-dependent friction coefficient was estimated using the following equation $B_3 = B_1 e^{\mu\beta}$, where B_3 and B_1 are the forces measured after and before the D-ring, respectively, β the angle between the belt sections in the D-ring and μ the friction coefficient. Although B_3 and B_1 were measured in the tests, the angle β was not measured. Therefore, this angle was estimated by performing a simulation for each ATD. These simulations used a constant friction coefficient of 0.14 and the angle between the belt sections was measured using the 3D animation of the simulation. Based on the simulation results, the final friction coefficient function defined for the simulations started at 0.14 and, after 40 ms, increased linearly to 0.18, reaching this value at 80 ms. This value was constant until the simulation finished.

Correlation Analysis

A visual correlation of the ATD's displacements was performed using the test recordings and simulations. All the signals measured in the test and simulation are shown in Table AI and Table AII in the Appendix. The correlation analysis was carried out according to [2][4][13]. The time window used for the correlation analysis was between t=0ms and the time of maximum head excursion in the x-axis + 20%, which was 120 ms. An ISO score was obtained for each channel used in the correlation by applying the ISO/TS 18571 [15]. When sensors measure more than one axis, e.g., linear accelerometers, they are grouped for correlation analysis by sensor. The sensor score was calculated as a weighted average of its channel scores using the following equation:

$$\boldsymbol{Score_{sensor} = \sum_i w_i * S_i \; with \; i = X,\; Y,\; Z,} \qquad \text{(Eq. 1)}$$

Where $\boldsymbol{S_i}$ is the score calculated for the channel in the $\boldsymbol{i}$-axis and $\boldsymbol{w_i}$ the weight for the channel, which was calculated using the following equation:

$$\boldsymbol{w_i = \frac{max\left(\left|Channel_{test_i}\right|\right)}{max\left(\left|Channel_{test_x}\right|\right)+max\left(\left|Channel_{test_y}\right|\right)+max\left(\left|Channel_{test_z}\right|\right)} \; with \; i = X,\; Y,\; Z,} \qquad \text{(Eq. 2)}$$

An additional comparison between the simulation and test results was carried out based on a set of injury criteria. This set of criteria was based on the frontal full-width impact from the adult occupant protection protocol by Euro

NCAP [1]. The results of the injury criteria were scaled by using a set of Injury Assessment Reference Values (IARVs), as the injury criteria values and magnitudes varied between them. The set of injury criteria and IARVs used in this study can be observed in Table I. The peak head acceleration and HIC were based on [1], and the other criteria were based on [16].

TABLE I
INJURY CRITERIA IARVS USED FOR COMPARING TEST AND SIMULATION RESULTS

Injury Criteria	H350M	H35F	H395M
HIC15	700	700	700
Acc3ms	80 g	80 g	80 g
Neck Fx	3.1 kN	1.95 kN	3.74 kN
Neck Fz (tension)	4.17 kN	2.62 kN	5.03 kN
Neck My (extension)	96 Nm	49 Nm	128 Nm
Chest Deflection	50 mm	41 mm	55 mm
Femur Fz	9.07 kN	6.16 kN	11.5 kN

III. RESULTS

A generic frontal impact sled FE model was developed to certify Hybrid III ATD FE models for use in virtual testing in frontal crashes.

Setting Up the Model to Test

Table II presents the H-point position and pelvis angles for each ATD size in both tests and simulation models, measured in the seat coordinate system. The H-point position in the x-axis and the pelvis angle showed the lowest deviation from the test measurements, as they were the main target of the positioning process.

The H-point position in the x-axis showed a deviation of less than 1 mm from the test mean for both the 50% and H35F ATDs. The position of the H-point in the z-axis showed a deviation ranging from 0 to 12 mm. To prevent vertical displacement at the beginning of the simulation, the H350M and H395M ATD models were positioned upwards compared to their physical counterparts, due to their shape-stiffness in the pelvis foam. Although the pelvis angles were within the standard deviation of the test measurements for the H35F and H395M ATD models, they deviated by 2 degrees from the mean for the H350M ATD model.

The H395M ATD model showed the largest deviation from the test mean measurements. Even though the initial positioning of the ATD was done following the test measurements, differences were observed between the ATD model and the 3D scanning. To investigate this, hard surfaces, i.e., neck discs, shoulder joints, knee joints, and shoes, and possible deviations in the positioning were considered. The final model position was obtained by excluding the H-point positioning tool and using other visible hard surfaces on the ATD, which resulted in a 12 mm deviation in the x-axis.

TABLE II
H-POINT POSITION AND HEAD AND PELVIS ANGLE MEASURED AT THE TESTS AND SIMULATIONS

Measurement	H350M		H35F		H395M	
	Test	Simulation	Test	Simulation	Test	Simulation
H-point x-axis position [mm]	-103±0	-102	-120±0	-120	-108±0	-96
H-point z-axis position [mm]	159±1	170	167±1	167	168±1	176
Pelvis angle [deg]	21.4±0.5	19.4	20.3±0.5	19.9	21.0±0.6	21.0

Fig. 3 shows pictures with an overlay of the simulation model in blue and the 3D scan of the physical ATD in red. The focus is on the head, thorax, arm, pelvis, and leg. Fig. 3a shows the head and neck of both the model and 3D scan. The nose tip was used as a control point to ensure that the model came in contact with the airbag at a similar time as the ATD in the tests. Fig. 3b shows a lateral view of the thorax and arms. The model's left arm was positioned mirroring the right arm, if there was any difference in the 3D scanning, to ensure symmetry. Fig. 3c shows the thorax and shoulder belt around the sternum. The belt path in the 3D scanning was used to ensure a belt fit similar to that in the simulation model. Fig. 3d and Fig. 3e show a lateral view of the pelvis and lower leg, respectively. Regarding the positioning of the lower extremities, the priority was to obtain a similar tibia angle and foot positioning, thus, the lower leg and feet were positioned using the 3D scan and the footrest was displaced until there was no penetration of the shoe sole as some differences were observed in between the

actual shoe sole and the one in the model.

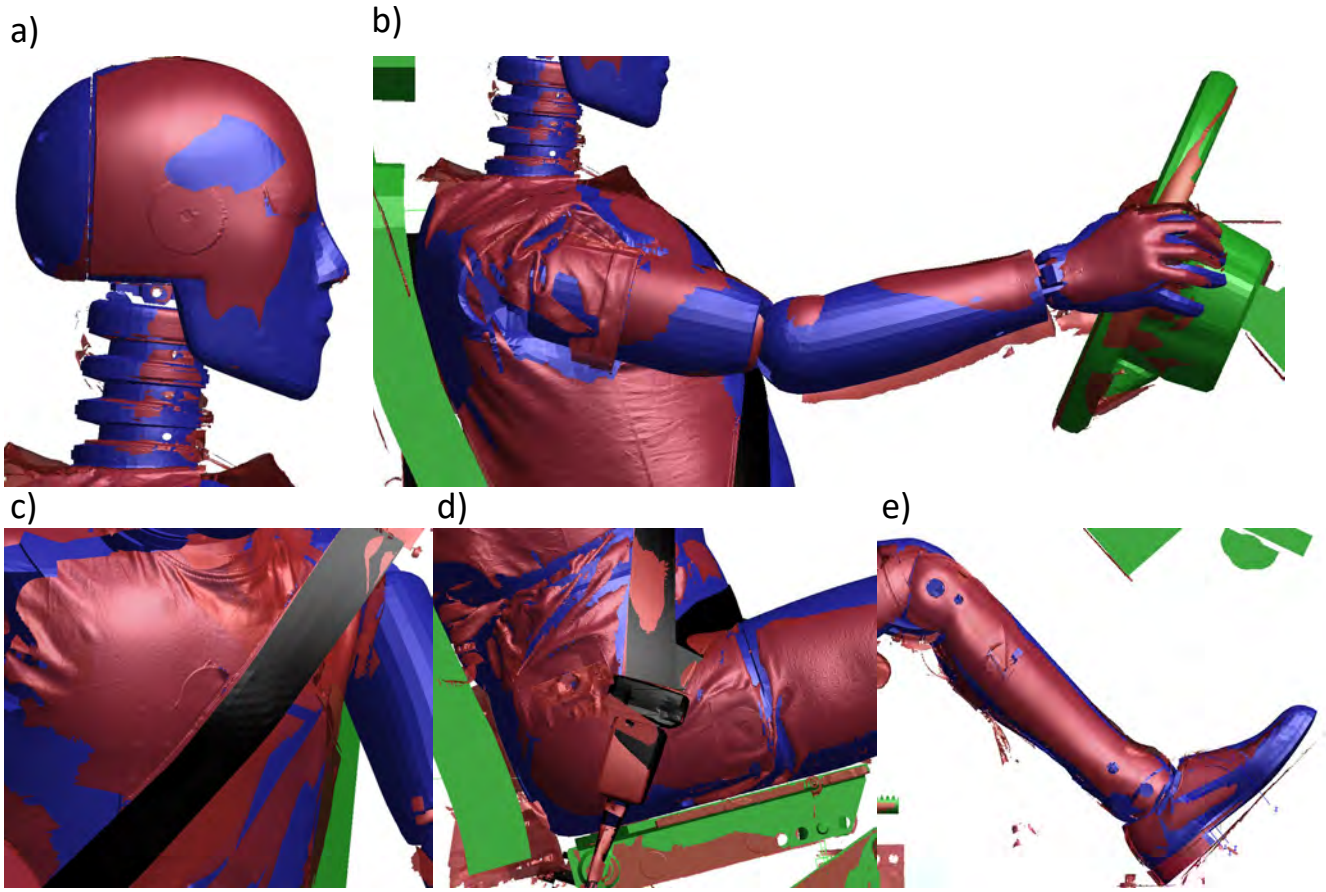

Fig. 3. Pictures of the 3D scanning overlaying the seated model for the H350M. a) Lateral view of the head; b) lateral view of the thorax and arms; c) view of the thorax and shoulder belt; and d) lateral view of the pelvis and buckle; lateral view of the lower leg.

Simulation Results

The simulation setups were assessed to ensure that the model fulfilled the quality criteria from [14] adapted to frontal impacts. These quality criteria were maximum hourglass energy < 10% of maximum internal energy, maximum hourglass energy of all H3 ATD components < 10% of maximum internal energy of H3 ATD, maximum mass added due to mass scaling to the total model is less than 5 % of the total model mass at the beginning of the run and less than 10 mm H-point z-displacement recorded in first 5 ms of the simulation. All these criteria were fulfilled by each setup.

Fig. A2 and Fig. A3 in the Appendix show the simulations using the 40 and 56 km/h full-frontal rigid barrier crash pulses, respectively, for each ATD at 0, 60, and 90 ms. The movements of the pelvis, thorax, and head showed hardly any differences in the human eye between the test and simulation outcomes. However, there were some discrepancies for the hands and forearms.

Correlation Results

A total of 18 tests were used as a reference for the correlation study between ATD sizes and crash pulses to ensure repeatability, i.e., three per test configuration. Fig. 4 shows the results for each ATD and crash pulse. The signals, which names are in the blue shadowed area, are boundary conditions, i.e., they do not belong to the ATD measurements. ATD accelerations, belt measurements and steering column force obtained a score above 0.6 in all simulations. The best correlation scores were observed for the belt measurements, with scores above 0.8 for all simulations. The mean standard deviation of the sensor scores within a test condition was 0.025. The mean absolute differences between the sensor scores for the two acceleration pulses were 0.056 for the H35F, 0.074 for the H350M and 0.076 for the H395M. Table III shows the mean scores for all the sensors in the simulation, for those that belong to the ATD and those that belong to the boundary conditions. The displacement of the steering column was not included in the latter group.

TABLE III
SENSOR SCORES OBTAINED FROM THE SIMULATIONS

	H350M		H35F		H395M	
	40 km/h	56 km/h	40 km/h	56 km/h	40 km/h	56 km/h
Mean simulation score	0.781 (±0.104)	0.810 (±0.082)	0.775 (±0.101)	0.786 (±0.115)	0.762 (±0.117)	0.757 (±0.128)
Mean ATD score	0.740 (±0.098)	0.783 (±0.074)	0.736 (±0.099)	0.738 (±0.12)	0.699 (±0.103)	0.692 (±0.123)
Mean boundary cond. Score (without steering column disp.)	0.841 (±0.082)	0.848 (±0.079)	0.832 (±0.075)	0.856 (±0.059)	0.852 (±0.064)	0.849 (±0.06)

The simulations for the H35F and H350M ATD models obtained the highest scores. The H395M showed a lower score in comparison to the other two ATDs, as a result of the mean ATD scores being lower. All the mean scores were larger for the 56 km/h full-frontal rigid barrier crash pulse relative to the 40 km/h full-frontal rigid barrier crash pulse, with the exception of the mean ATD score of the H395M. When focusing on just the sensor scores for all ATD, the lowest scores were observed for the neck and lumbar spine forces and moments.

When focusing on sensors that belonged to the boundary conditions, the scores were equal to or above 0.8 for all three ATDs. Belt forces and webbing pay-in and pull-out were the channels with the largest scores (all above 0.8). The displacement of the steering column showed the lowest correlation scores, within the range of 0.2 and 0.4 for the 40 km/h full-frontal rigid barrier crash pulse and above 0.6 for the 56 km/h full-frontal rigid barrier crash pulse. Although the correlation score was below 0.4 for the 40 km/h full frontal rigid barrier crash pulse, the difference in the displacement of the steering column was 2 mm. Although a difference was observed using the 56 km/h full frontal rigid barrier crash pulse, the correlation score method resulted in a lower score due to the low deflection magnitudes in the 40 km/h full frontal rigid barrier crash pulse case.

Fig. 5 shows the normalised injury criteria measured in the tests and simulation for the frontal crash using a 40 and 56 km/h full-frontal rigid barrier crash pulse. The mean difference between the test and the predictions with the simulations was 0.055 of the normalised injury criteria, i.e., 5.5% of the IARVs. Injury criteria with the largest discrepancies were neck forces and moment for all ATDs, and HIC15 and chest deflection for specific ATDs.

Peak neck shear forces were overpredicted by 8 to 13% of the IARVs. This difference between the simulations and tests was attributed to the initial airbag interaction with the head. The interaction with the airbag also resulted in a larger peak neck bending moment compared with the measurements from the tests, which resulted in a 2 to 18% of the IARV difference. Peak neck force in the z-axis was underpredicted by the H35F ATD when using both acceleration pulses. These differences in the peak neck force in the z-axis ranged from 9 to 12% of the IARV.

Although a small difference was observed in peak chest deflection between physical and virtual H350M and H35F ATDs, i.e., 1 to 4% of the IARV, the H395M ATD under-predicted peak chest deflection when using both crash pulses with differences that range from 7 to 12% of the IARV.

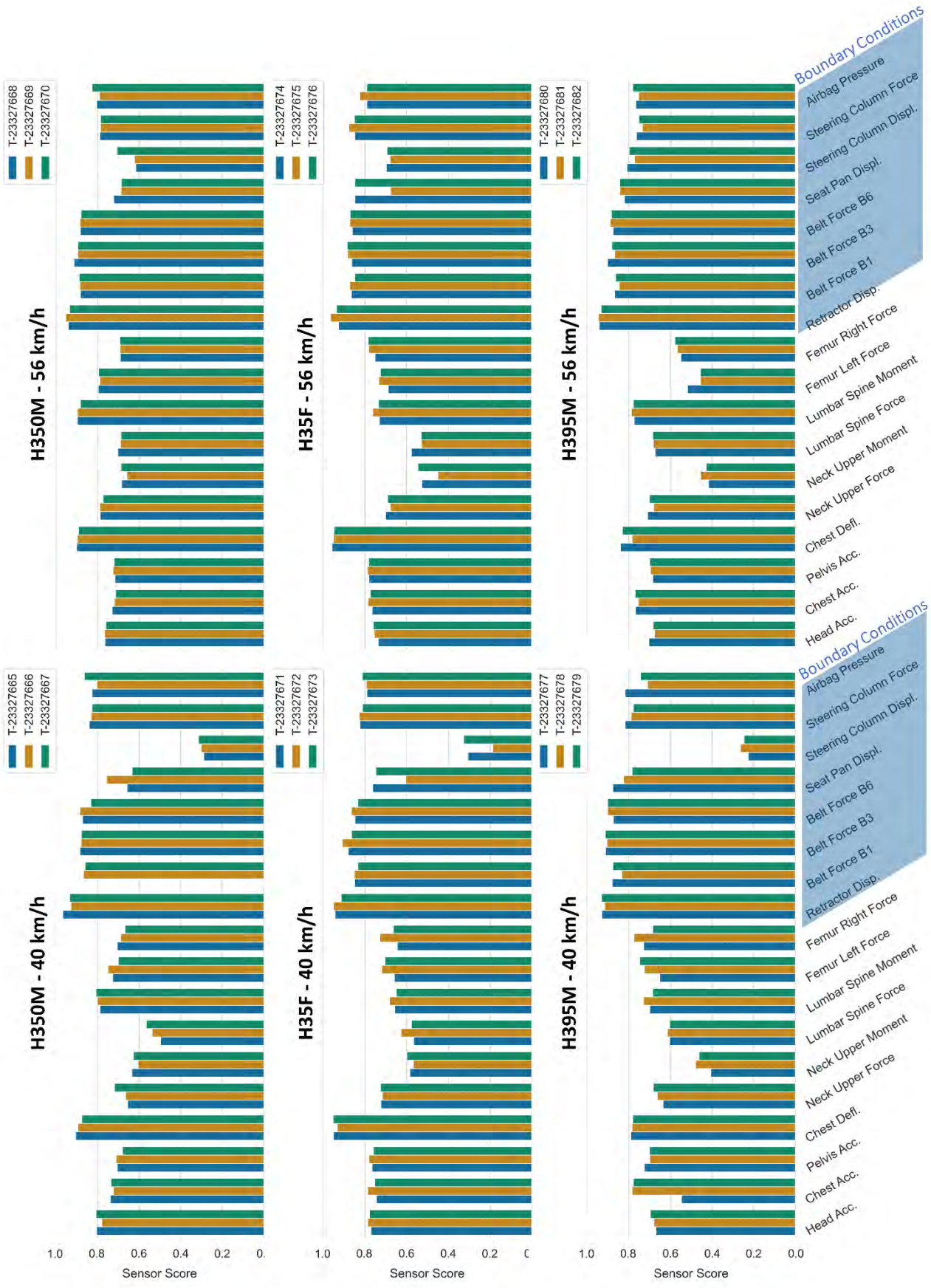

Fig. 4. Sensor correlation scores for the family of H3 adult ATDs between three tests and the simulation model in a frontal crash with a 40 and 56 km/h full-frontal rigid barrier crash pulse.

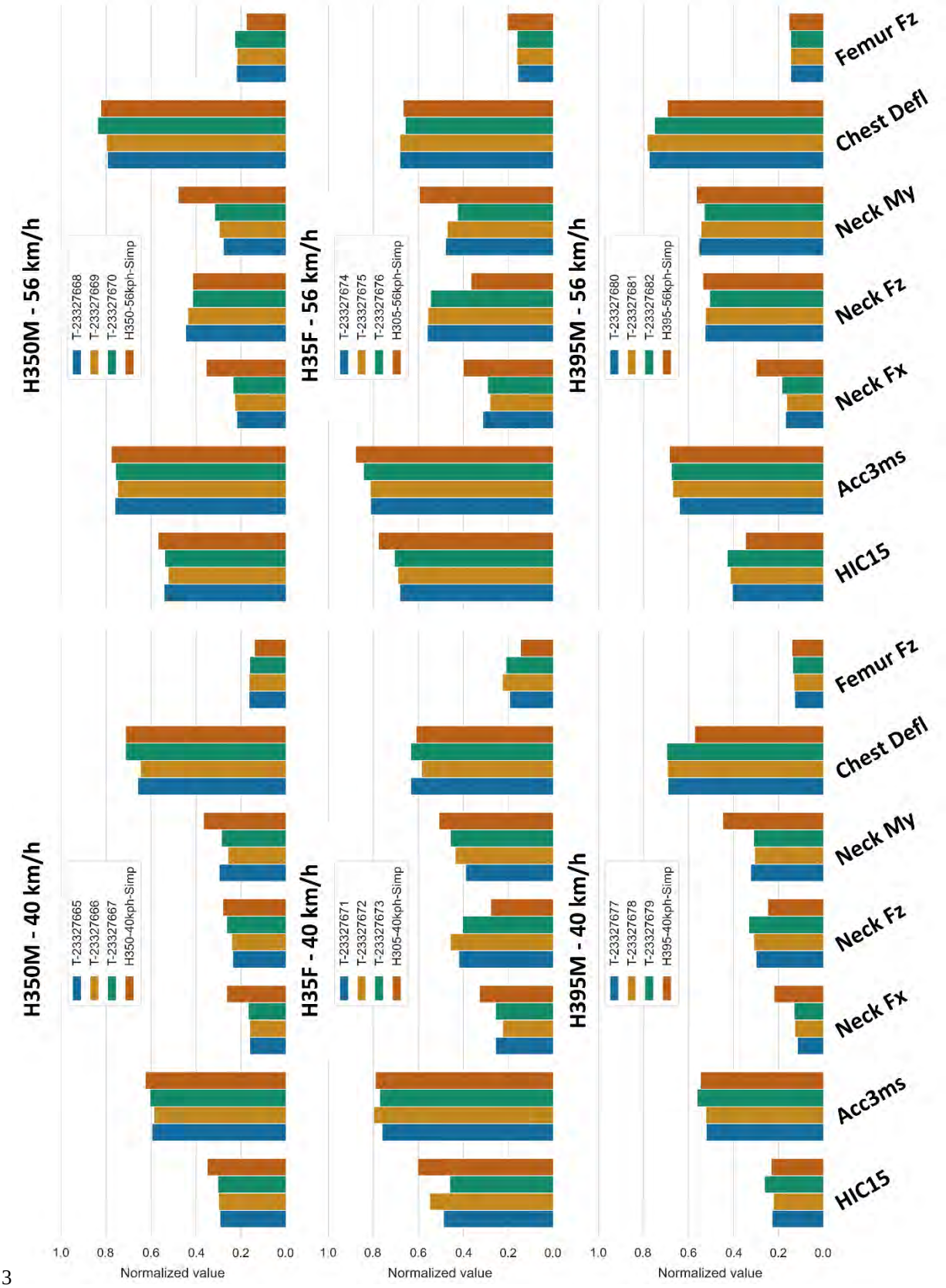

Fig. 5. Normalised injury criteria for the family of H3 adult ATDs between three tests and the simulation model in a frontal crash with a 40 and 56 km/h acceleration pulse.

IV. DISCUSSION

An open-source generic frontal impact sled FE model and a method, which can be used in full-body certification of the family of adult H3 ATD FE models to be used for Virtual Testing in frontal crashes, were developed. The performance of the generic frontal impact sled FE model was comparable to that of the generic

far-side impact sled model [4]. To enable the development of a model qualification procedure, the results from the tests [8] and the model described in this study have been made available on the openvt.eu platform.

Although the H395M showed the largest deviation from the pelvis measurements, i.e., h-point position and pelvis angle, the surface of the model matched the 3D scanning, repeating the positioning process. It was hypothesised that a small rotation of the pelvis around the vertical axis could have resulted in observed deviations, as only one H-point positioning tool was used with this ATD. To check this hypothesis, the angle required to obtain a 12 mm deviation was calculated using the length of the positioning tool (approx. 287 mm from the H-point), which resulted in 2 to 2.5 degrees. This was considered within the range of deviation in the test since only one H-point positioning tool was used. To reduce these uncertainties, the use of the H-point positioning tool on both sides of the ATD pelvis was recommended in future testing.

A fair overall correlation, i.e., 0.58<score≤0.8 [10], was obtained from the model. While lower scores were observed for the neck, lumbar and femur sensors for some configurations, i.e., combination of ATD and acceleration pulse, the injury criteria measured with these sensors were below 50% of their IARV. The H395M ATD showed the largest differences in chest deflection relative to the tests. Thus, the video recordings were analysed to check for any variations in the thorax motion. This analysis revealed that the jacket around the left shoulder was not deforming in the same way as observed in the tests. This could have resulted in a different shoulder belt-to-chest interaction and, therefore, a different reading in the displacement of the chest deflection sensor. A good correlation, i.e., 0.8<score≤0.94 [10], was obtained in all cases for the sled measurements.

When focusing on each specific ATD, the H350M and H35F ATD models obtained the best match between the scaled injury criteria and the highest correlation scores. Both models have been used or are in use for vehicle crashworthiness assessment by public or private entities around the world. Thus, the higher correlation score of these models could be related to their use by the industry in the development of their products, which could potentiate the development of these models. These can be observed in the release versions of the ATD models, where the H350M and H35F ATD model release versions were 1.5.1 and 2.0.2, while the H395M ATD model release version was 1.0.2.

In the 56 km/h tests and models, it was observed that the steering column and seat pan strokes bottomed out for the H395 ATD. Regarding the steering column stroke, neither the test nor the simulation showed an increase in bag pressure due to the steering column bottoming out. However, capturing the time of the steering column stroke and its associated peak force may prove challenging, as the simplified model does not fully represent the clearances and deformation of all the elements of its physical counterpart. Therefore, when developing the certification method this signal may be excluded to avoid nonlinear effects.

The seat pan's influence on the test results was considered found to be negligible in the physical tests. However, in the model, the influence was greater, resulting in a larger acceleration peak at the pelvis. To prevent bottoming out for the H395M ATD in future testing, redesigning the generic seat to make the available seat pan stroke longer may be necessary.

The development of this open-source generic frontal impact sled model was not exempt from limitations. A total of 18 tests were conducted, with three tests for each configuration to ensure reproducibility. However, only one ATD was used for each size, which meant that the reproducibility of the ATD due to its manufacturing process, i.e., variations within the manufacturing tolerances, was not considered. Thus, tests with other ATDs could be used to enhance the certification process. Variations in the sled model could also be introduced in the future to enhance the robustness of the ATD certification process. While the generic seat used in the study did not represent any specific seat, it was designed with a rigid seat pan and anti-submarining pan. Including a set of tests with a deformable seat, closer to the vehicle environment used for VTC, could enhance the ATD certification process. Furthermore, additional different seatbelt and airbag configurations can be implemented to represent the variations in the vehicle fleet.

V. CONCLUSIONS

An open-source generic frontal impact sled FE model was developed that can be used in a certification procedure for Hybrid III adult ATD models to be used in Virtual Testing in a frontal crash. Therefore, new Hybrid III ATD FE models or future improvements implemented in current models could be certified using this model. This is a crucial step towards the Euro NCAP 2030 roadmap, where Virtual Testing using the Hybrid III adult ATD

FE models is planned to be implemented. The open-source generic frontal impact sled FE-model's correlation showed similar results as those observed for the Euro NCAP far-side impact ATD certification model.

VI. ACKNOWLEDGEMENT

The authors would like to acknowledge the contribution of Mikael Dahlgren, Mikael Videby, and Mohan Jayathirtha for their assistance in resolving issues related to the positioning of the ATD models.

VII. REFERENCES

[1] Euro NCAP. (2023) Euro NCAP, European New Car Assessment Programme, *Assessment Protocol – Adult Occupant Protection - Implementation 2024 - v9.3*, Belgium.

[2] Putzer, M., Adamou, F.E.N., Zhu, F., Walz, M., and Galazka, J. (2023) A process to qualify a dummy model for the use in a virtual testing application. *Proceedings of Conference 27th ESV Conference*, 2023, Yokohama, Japan.

[3] Klug, C., Feist, F., Schneider, B., Sinz, W., Ellway, J., and van Ratingen, M. (2019) Development of a certification procedure for numerical pedestrian models. *Proceedings of Conference 26th ESV Conference*, 2019, Eindhoven, Netherlands.

[4] Klug, C., Schachner, M., et al. (2023) Euro NCAP virtual testing-crashworthiness. *Proceedings of Conference 27th ESV Conference*, 2023, Yokohama, Japan.

[5] Euro NCAP VTC Group (2023) Euro NCAP *Qualification Procedure for Virtual Dummy Models Part 1: WorldSID AM50 1.0,* Belgium.

[6] Shah, C., Khambati, S., Brock Watson, N.B., Zhou, Z., Zhu, F., and Shetty, S. (2014) Newly developed LS-DYNA® models for the THOR-M and harmonized HIII 50th crash test dummies. *Proceedings of Conference Proceedings of the 13th International LS-DYNA Users Conference*, 2014, Michigan, United States.

[7] Mohan, P., Park, C.-K., et al. (2010) LSTC/NCAC dummy model development. *Proceedings of Conference 11th International LS-Dyna Users Conference*, 2010, Detroit, United States.

[8] Pipkorn, B., Valdano, M., Östling, M., Eriksson, L., Videby, M., and Lopez-Valdes, F. (2024) Sled Tests for Development of HIII Dummy Certification Method (in review). *Proceedings of Conference Proceedings of the IRCOBI Conference*, 2024, Stockholm, Sweden.

[9] Höschele, P., Smit, S., Tomasch, E., Östling, M., Mroz, K., and Klug, C. (2022) Generic crash pulses representing future accident scenarios of highly automated vehicles. SAE International Journal of Transportation Safety, **10**(2): p.185–210.

[10] International Organization for Standardization (2014) ISO/TS 18571: 2014, *Road Vehicles—Objective rating metric for non-ambiguous signals,* Geneva, Switzerland.

[11] Uriot, J., Potier, P., et al. (2015) Reference PMHS Sled Tests to Assess Submarining. Stapp Car Crash Journal, **59**: p.203–223.

[12] Östling, M., Eriksson, L., Dahlgren, M., and Forman, J. (2023) Frontal head-on car-to-heavy goods vehicle crashes effect on the restraint system. *Proceedings of Conference 27th ESV Conference*, 2023, Yokohama, Japan.

[13] Dahlgren, M., Vishwanatha, A., Soni, A., Engstrand, K., Forsberg, J., and Yeh, I. (2020) Belt modelling in LS-DYNA®. *Proceedings of Conference 16th International LS-DYNA Users Conference*, 2020, Virtual Event.

[14] Euro NCAP. (2023) Euro NCAP, *Virtual Far Side Simulation & Assessment Protocol - Implementation 2024 - v1.0*, Belgium.

[15] Graz University of Technology. "Validation-Metrics / Objective Rating Metric ISO 18571 · GitLab", https://openvt.eu/validation-metrics/ISO18571. [accessed 2/22/2024].

[16] Mertz, H.J., Irwin, A.L., and Prasad, P. (2003) Biomechanical and Scaling Bases for Frontal and Side Impact Injury Assessment Reference Values. Stapp Car Crash Journal, **47**: p.155–188.

VIII. APPENDIX

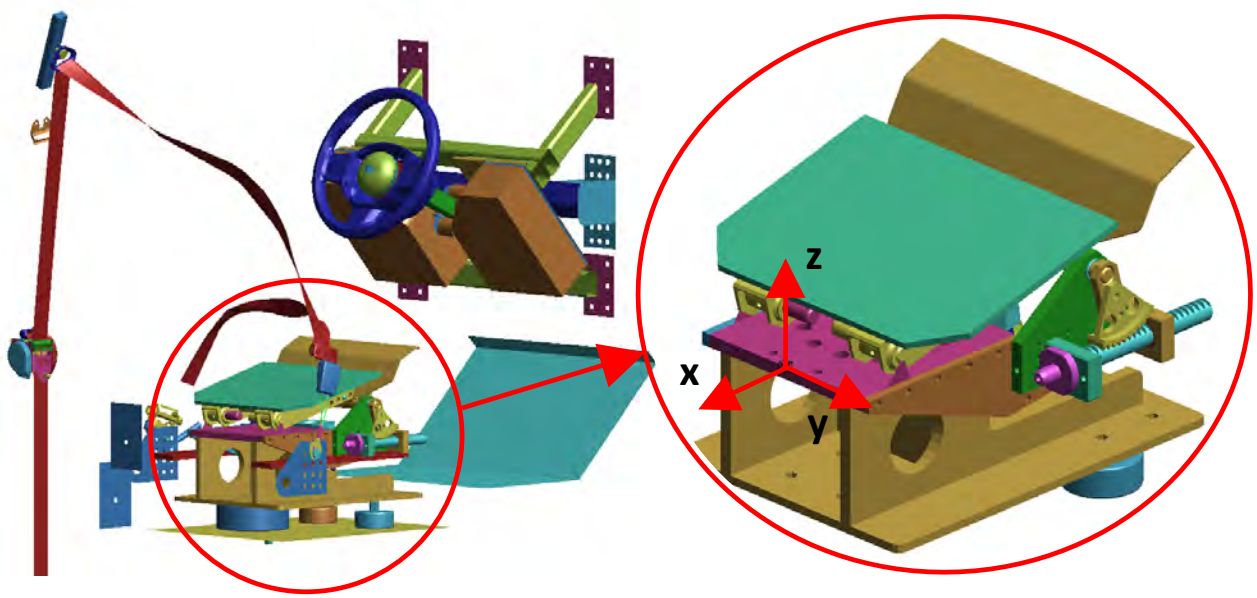

Fig. A1. Seat coordinate system used to measure ATD position.

TABLE AI
ATD AND BOUNDARY CONDITIONS CHANNELS AND SENSORS MEASURED IN THE TEST AND SIMULATION MODEL. THE FILTER WAS USED TO DISPLAY THE SIGNALS READING IN FIG. TO FIG. .

Sensor	Channel	Filter	Used for correlation	Tmin [ms]	Tmax [ms]	Measured in test
Head acceleration	X axis	CFC1000	TRUE	0	120	TRUE
	Y axis	CFC1000	TRUE	0	120	TRUE
	Z axis	CFC1000	TRUE	0	120	TRUE
Chest acceleration	X axis	CFC180	TRUE	0	120	TRUE
	Y axis	CFC180	TRUE	0	120	TRUE
	Z axis	CFC180	TRUE	0	120	TRUE
Pelvis acceleration	X axis	CFC1000	TRUE	0	120	TRUE
	Y axis	CFC1000	TRUE	0	120	TRUE
	Z axis	CFC1000	TRUE	0	120	TRUE
Chest deflection	-	CFC600	TRUE	0	120	TRUE
Upper neck force	X axis	CFC1000	TRUE	0	120	TRUE
	Y axis	CFC1000	TRUE	0	120	TRUE
	Z axis	CFC1000	TRUE	0	120	TRUE
Upper neck moment	X axis	CFC600	TRUE	0	120	TRUE
	Y axis	CFC600	TRUE	0	120	TRUE
	Z axis	CFC600	TRUE	0	120	TRUE
Lumbar spine force	X axis	CFC600	TRUE	0	120	TRUE
	Y axis	CFC600	FALSE	0	120	FALSE
	Z axis	CFC600	TRUE	0	120	TRUE
Lumbar spine moment	X axis	CFC600	FALSE	0	120	FALSE
	Y axis	CFC600	TRUE	0	120	TRUE
	Z axis	CFC600	FALSE	0	120	FALSE
Femur left force	Z axis	CFC600	TRUE	0	120	TRUE
Femur right force	Z axis	CFC600	TRUE	0	120	TRUE

TABLE AII

CHANNELS AND SENSORS MEASURED IN TEST AND SIMULATION MODEL

THE FILTER WAS USED TO DISPLAY THE SIGNALS READING IN FIG. A4 TO FIG. A9.

Sensor	Channel	Filter	Used for correlation	Tmin [ms]	Tmax [ms]	Measured in test
Belt a pay-in and pull- out	-	*CFC180*	*TRUE*	*0*	*120*	*TRUE*
Belt force at retractor (B1)	-	*CFC600*	*TRUE*	*0*	*120*	*TRUE*
Belt force at shoulder (B3)	-	*CFC600*	*TRUE*	*0*	*120*	*TRUE*
Belt force at end bracket (B6)	-	*CFC600*	*TRUE*	*0*	*120*	*TRUE*
Seat pan displacement	-	*CFC180*	*TRUE*	*0*	*120*	*TRUE*
Steering column displacement	-	*CFC060*	*TRUE*	*0*	*120*	*TRUE*
Steering column force	-	*CFC060*	*TRUE*	*0*	*120*	*TRUE*
Airbag Pressure	-	*CFC180*	*TRUE*	*20*	*120*	*TRUE*

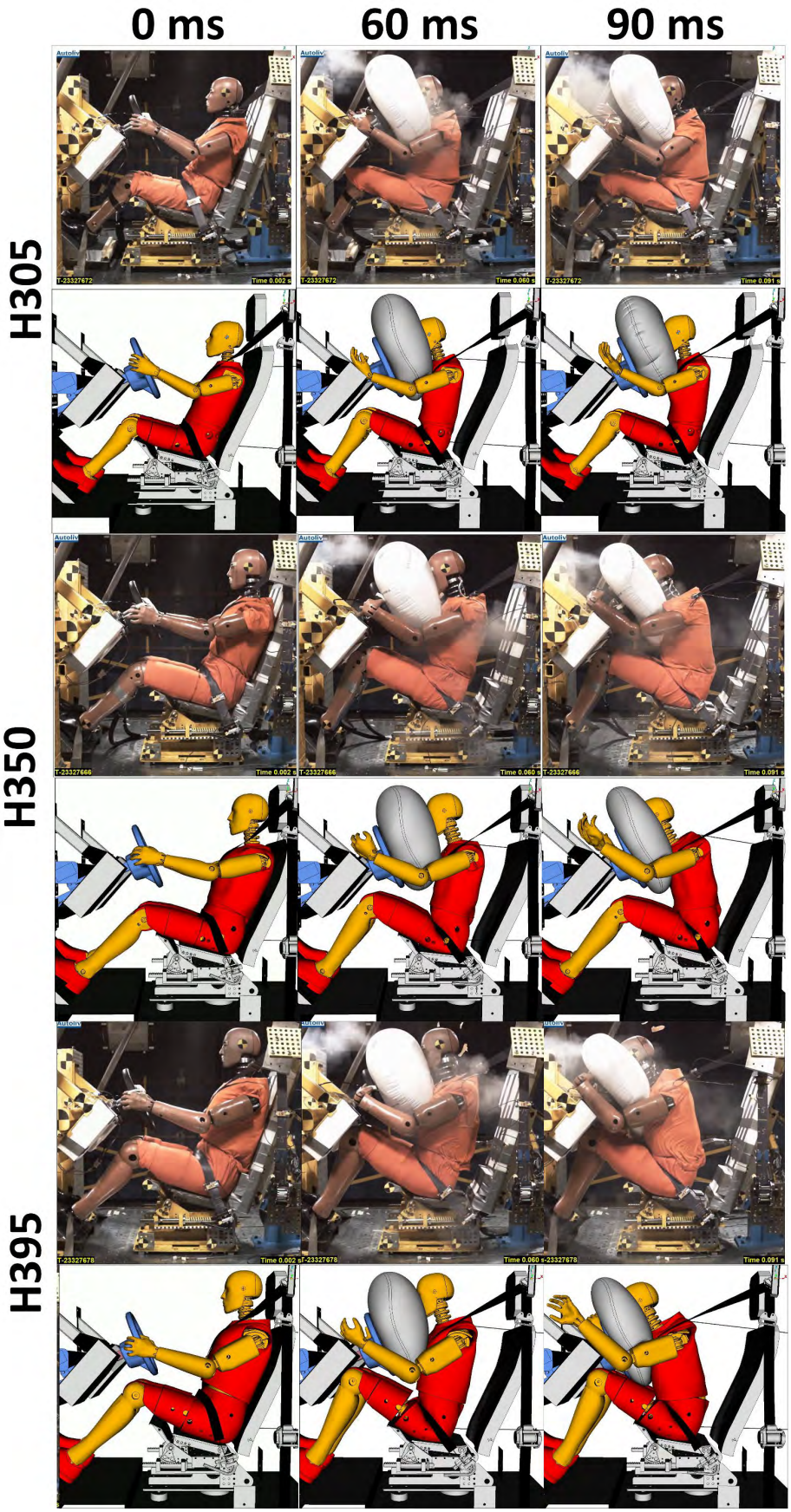

Fig. A2. Physical test and simulation model pictures using the 40 km/h acceleration pulse. First, second and third columns show pictures at 0, 60 and 90 ms of the acceleration pulse. First two rows show the H350M ATD in the physical test and simulation, respectively. Next rows show the tests and simulation for the H35F and H395M ATDs.

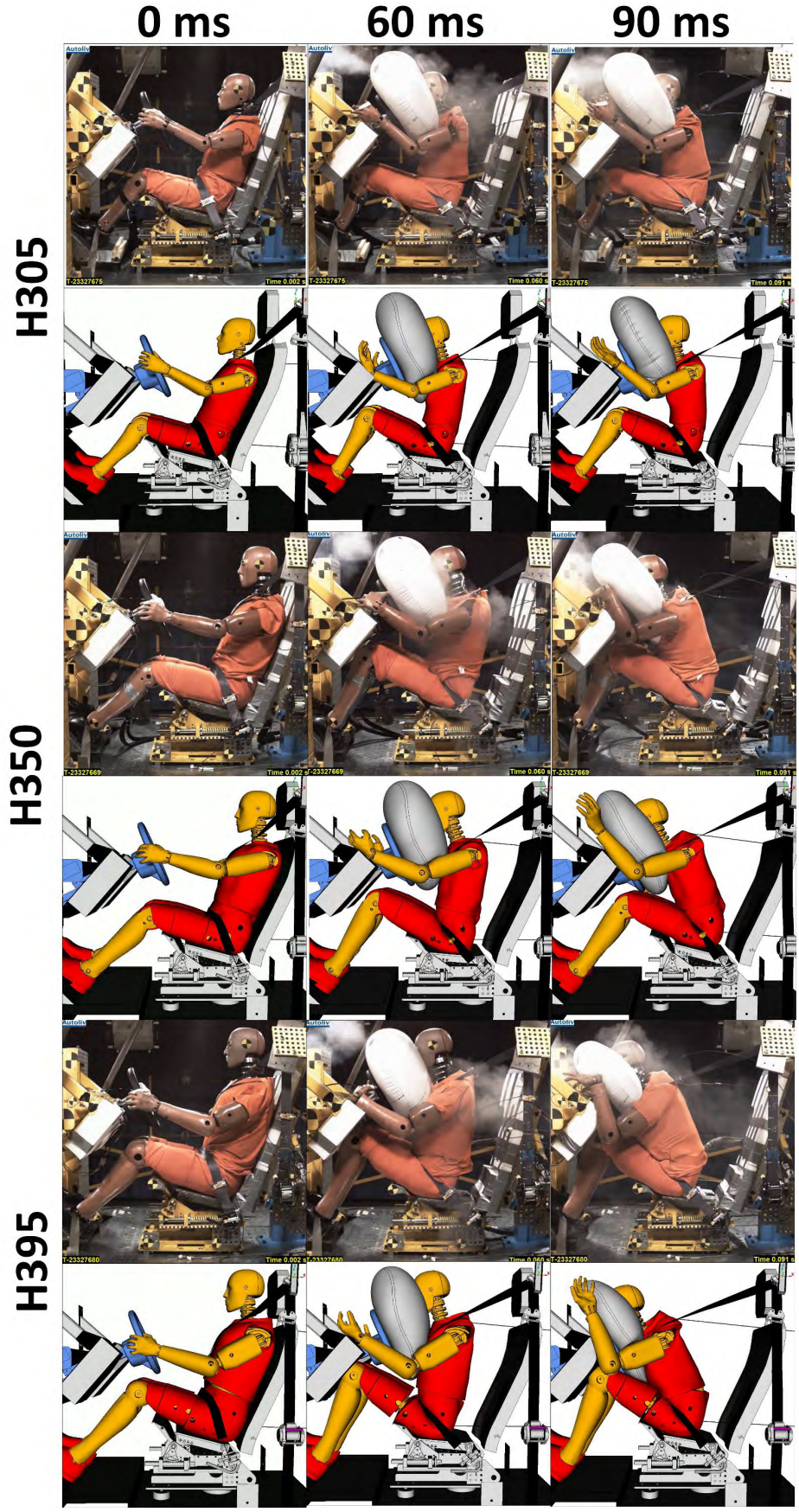

Fig. A3. Physical test and simulation model pictures using the 56 km/h acceleration pulse. First, second and third columns show pictures at 0, 60 and 90 ms of the acceleration pulse. First two rows show the H350M ATD in the physical test and simulation, respectively. Next rows show the tests and simulation for the H35F and H395M ATDs.

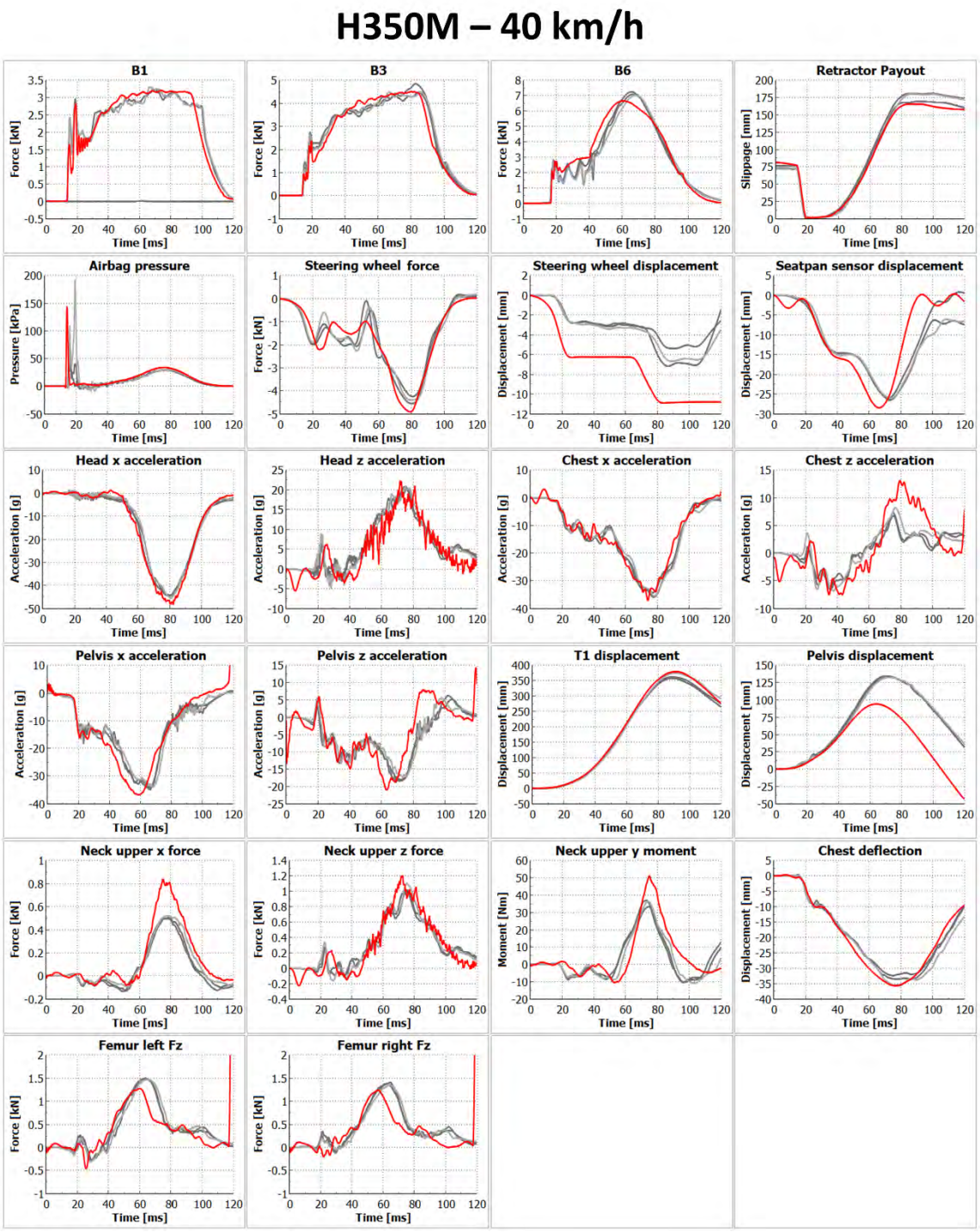

Fig. A4. H350M ATD measurements from the tests and simulations for the 40 km/h impact velocity case. Tests measurements in grey and simulation measurements in red.

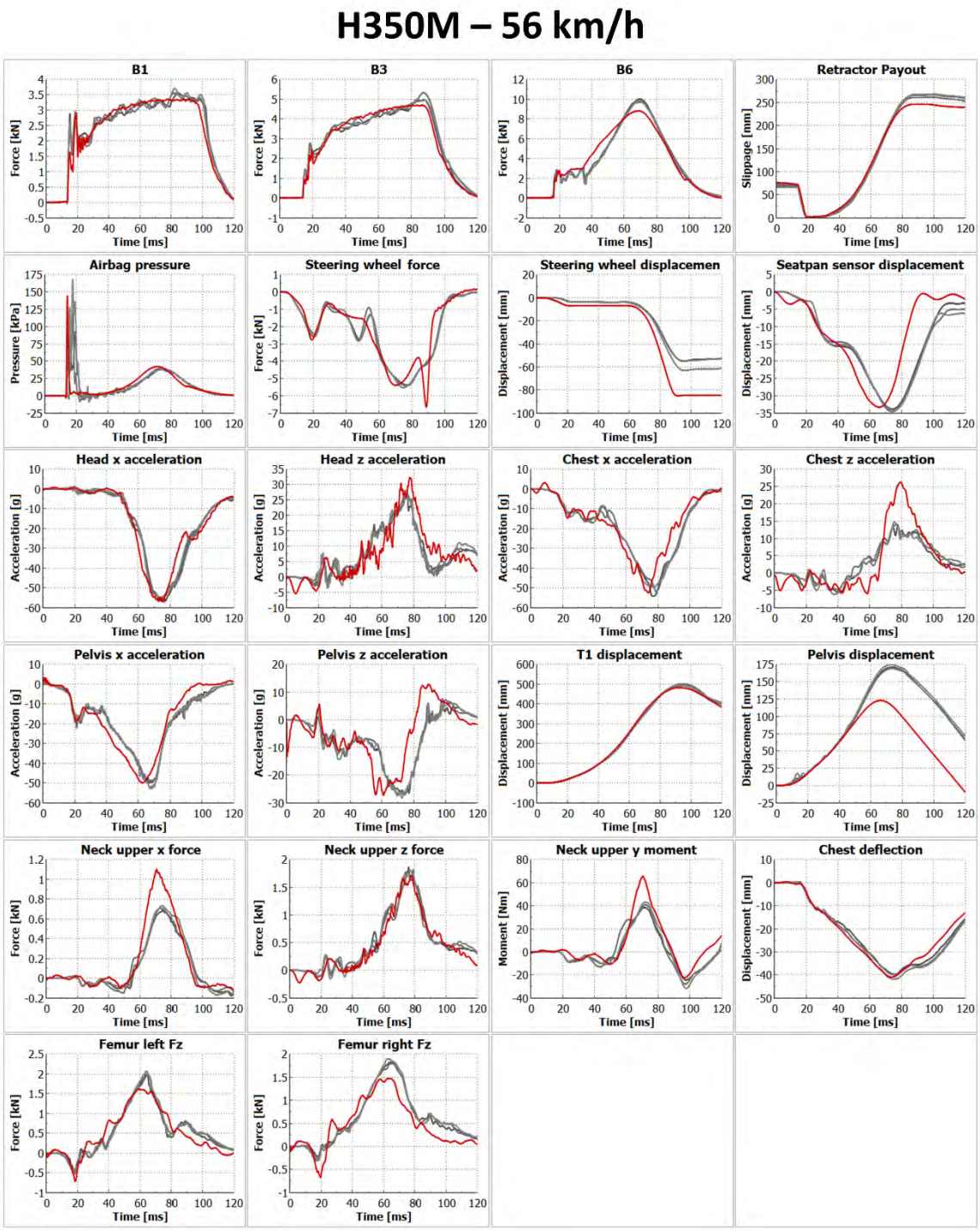

Fig. A5. H350M ATD measurements from the tests and simulations for the 56 km/h impact velocity case. Tests measurements in grey and simulation measurements in red.

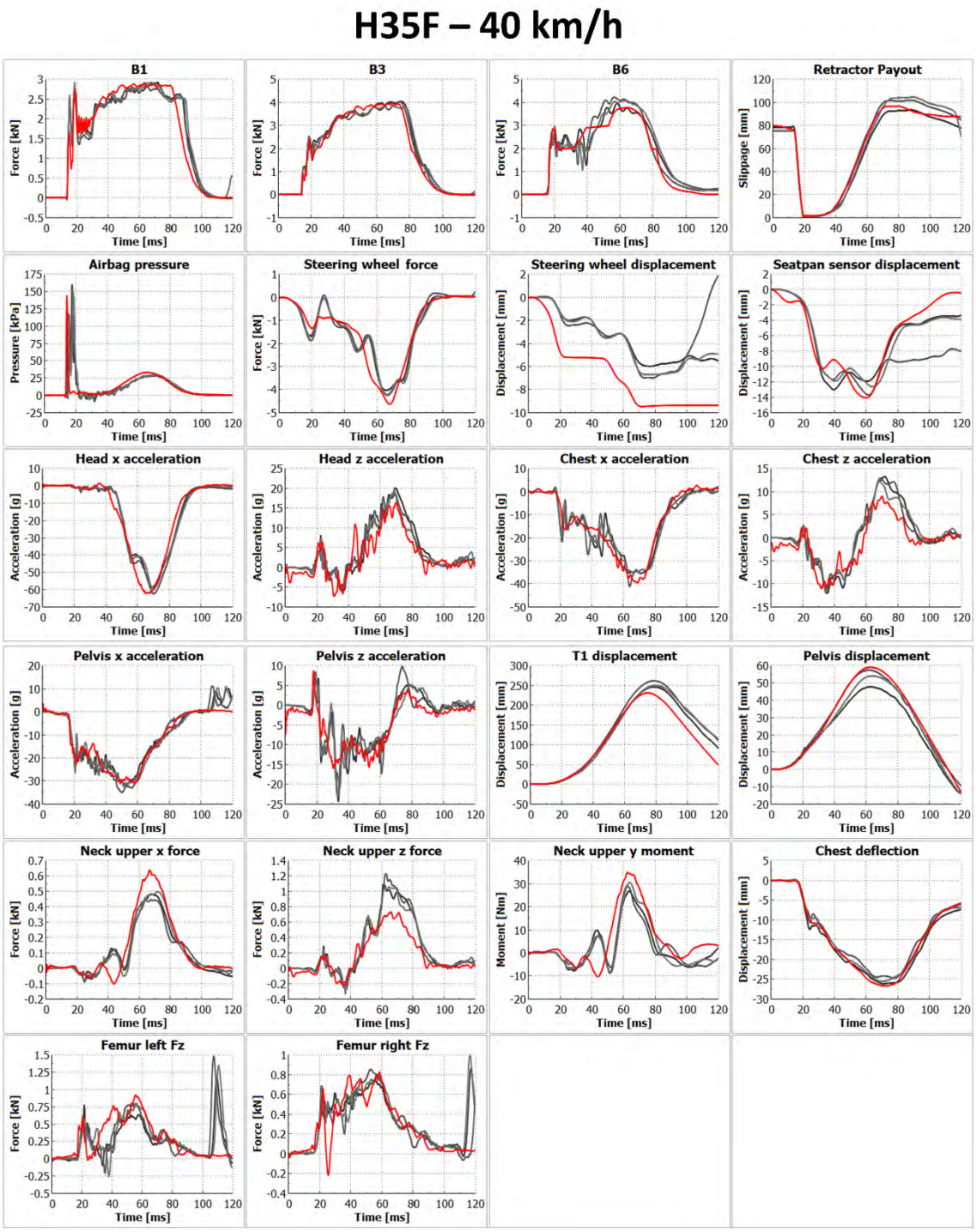

Fig. A6. H35F ATD measurements from the tests and simulations for the 40 km/h impact velocity case. Tests measurements in grey and simulation measurements in red.

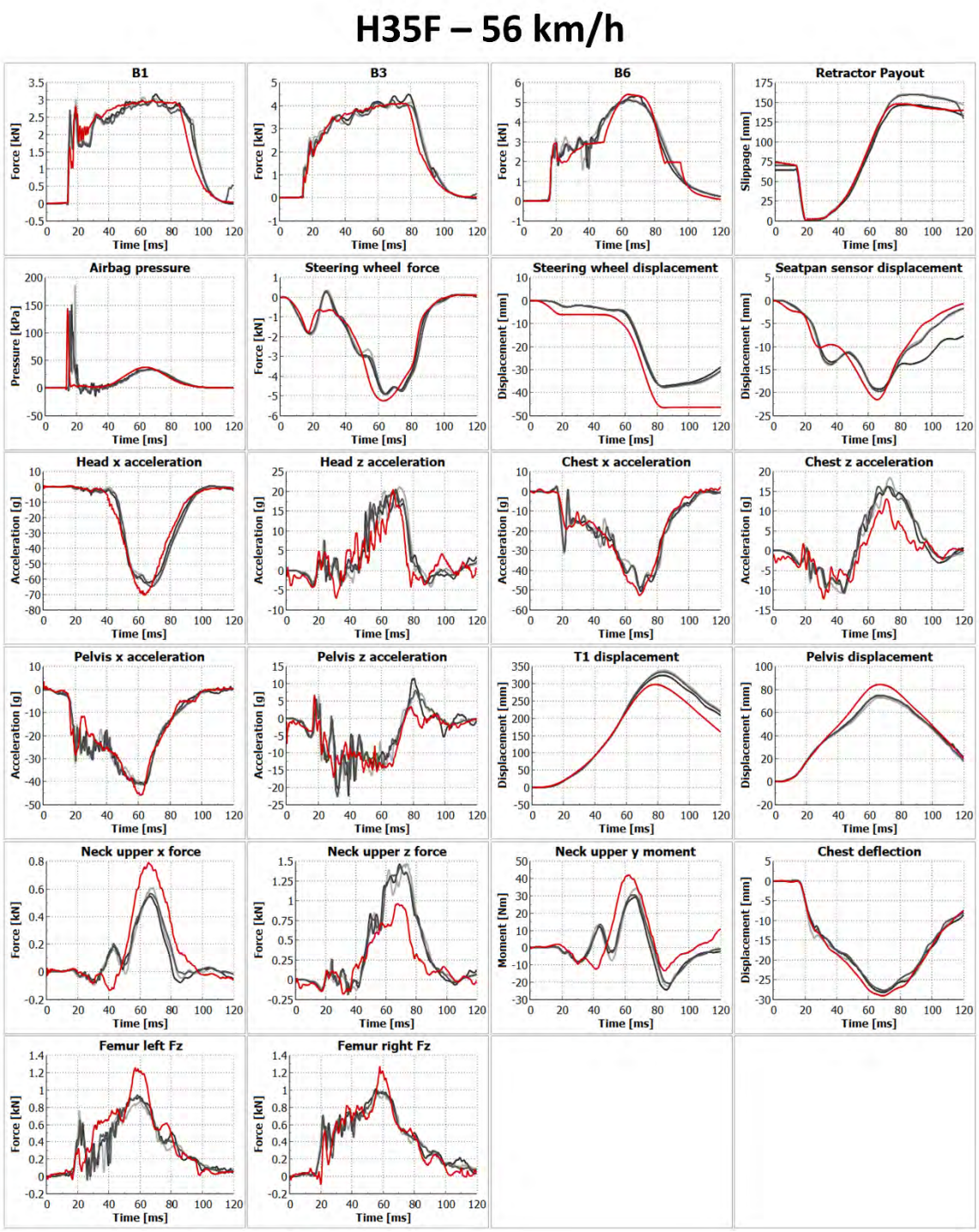

Fig. A7. H35F ATD measurements from the tests and simulations for the 56 km/h impact velocity case. Tests measurements in grey and simulation measurements in red.

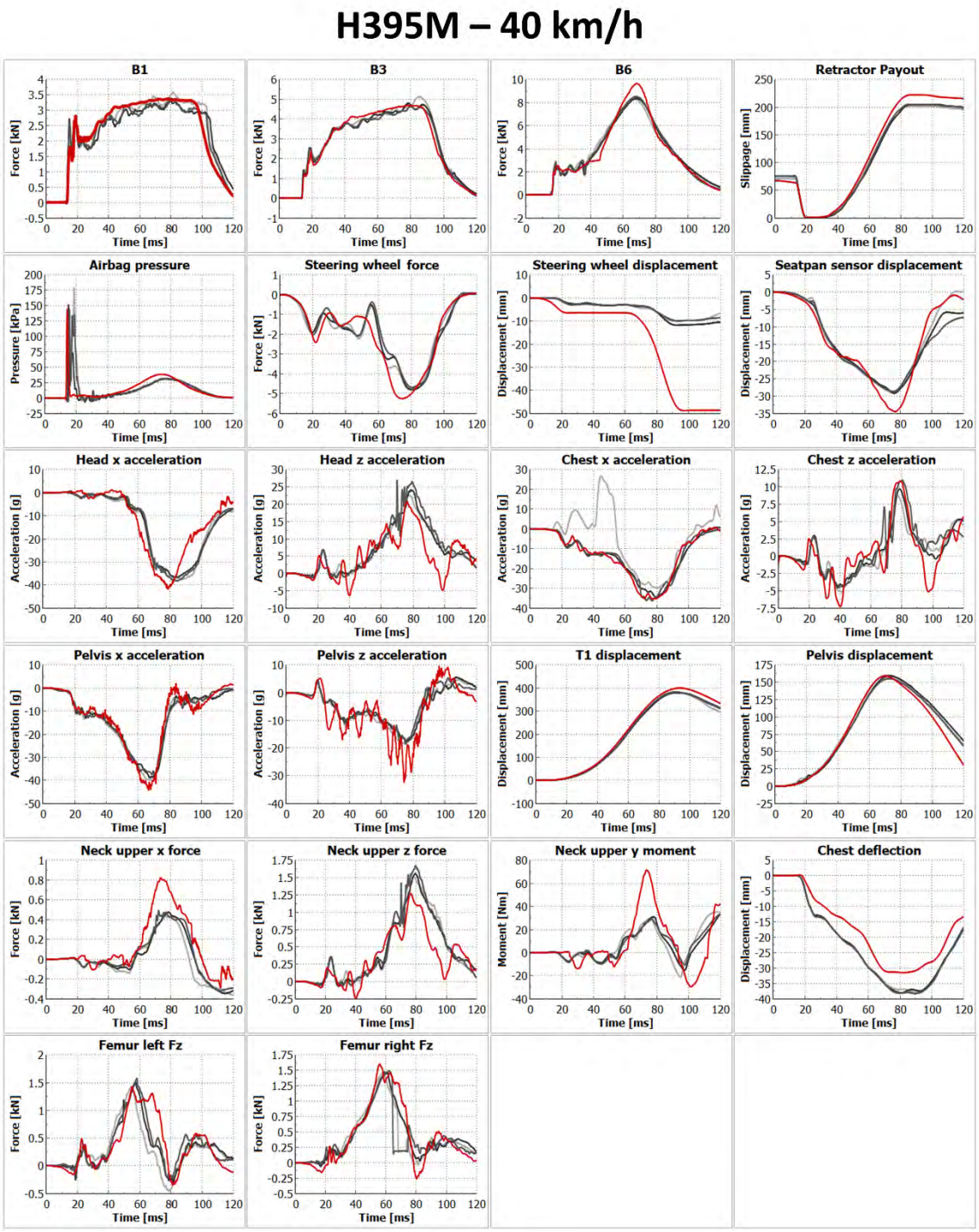

Fig. A8. H395M ATD measurements from the tests and simulations for the 40 km/h impact velocity case. Tests measurements in grey and simulation measurements in red.

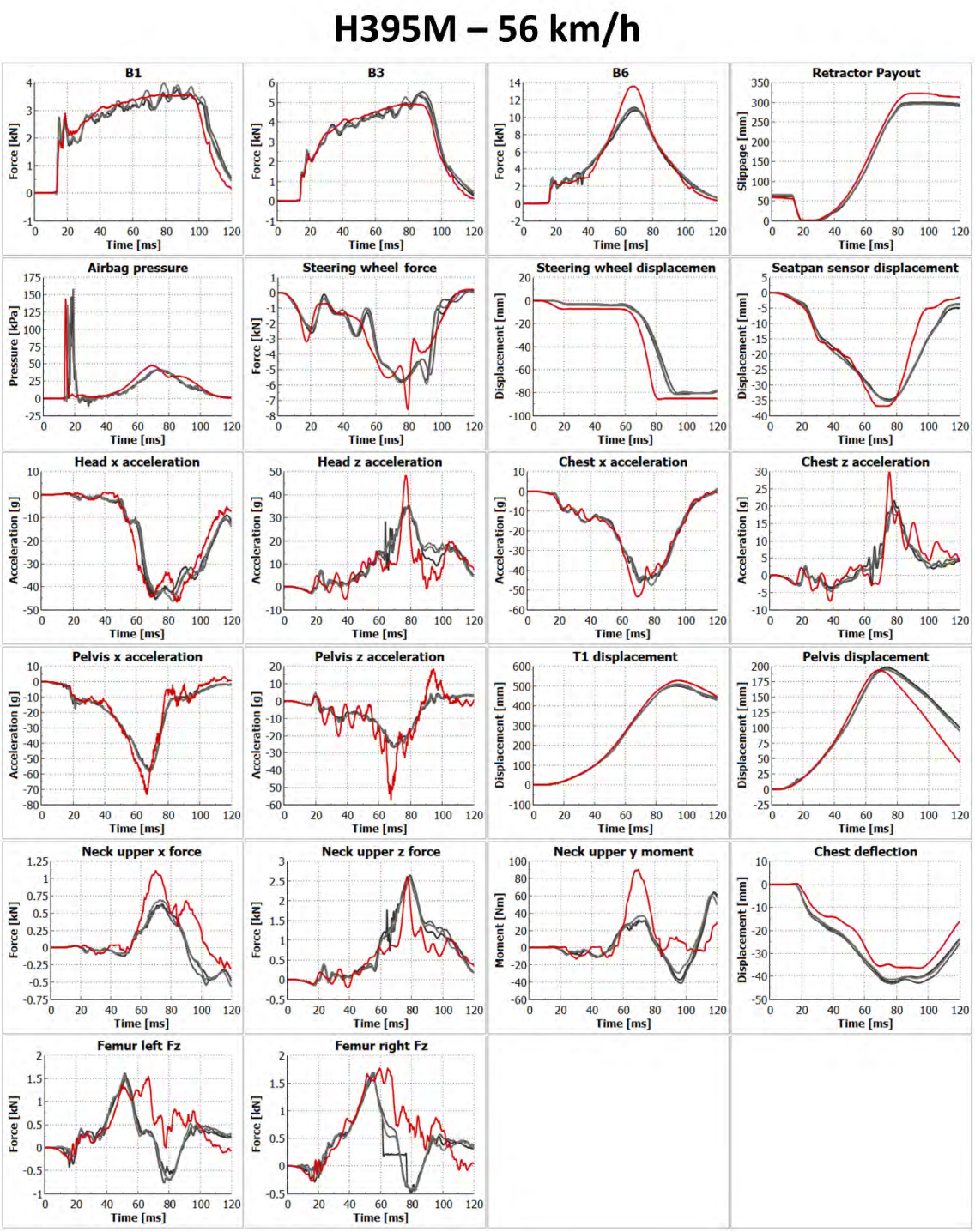

Fig. A9. H395M ATD measurements from the tests and simulations for the 56 km/h impact velocity case. Tests measurements in grey and simulation measurements in red.